Nauplius
THE JOURNAL OF THE BRAZILIAN CRUSTACEAN SOCIETY

e-ISSN 2358-2936
www.scielo.br/nau
www.crustacea.org.br

ORIGINAL ARTICLE

Two new species of freshwater crabs of the genus *Potamiscus* Alcock, 1909 (Brachyura: Potamidae) from Nagaland, northeastern India

Sameer Kumar Pati orcid.org/0000-0001-8418-7500

Zoological Survey of India, Western Regional Centre. Vidyanagar, Sector 29, P.C.N.T. Post, Akurdi, Pune-411 044, Maharashtra, India.

ZOOBANK: http://zoobank.org/urn:lsid:zoobank.org:pub:F92DC3E0-CA81-4221-AC51-810D8337B17F

ABSTRACT

Two new species of freshwater crabs of the potamid genus *Potamiscus* Alcock, 1909 are described from Nagaland State of northeastern India. *Potamiscus chizami* sp. nov. and *Potamiscus mima* sp. nov. most resemble two Indian congeners [*Potamiscus palelensis* Mitra and Waikhom, 2019 and *Potamiscus tumidulus* (Alcock, 1909)] and a species from Myanmar (*Potamiscus whitteni* Ng, Hla Htoo and Win Mar, 2020) due to the similar terminal segment of the male first gonopod. Both new species can be distinguished from *Po. palelensis* by their stouter ambulatory legs, from *Po. tumidulus* by their more-slender male first gonopod, and from *Po. whitteni* by their strongly concave lateral margins of the male telson and the straight tip of the male first gonopod. Characters of the carapace, male pleon, male gonopods, and female vulvae are employed to differentiate *Po. chizami* sp. nov. from *Po. mima* sp. nov.

KEYWORDS

Crustacea, Decapoda, description, Potamiscinae, taxonomy

INTRODUCTION

The freshwater crab genus, *Potamiscus* Alcock, 1909, of the family Potamidae Ortmann, 1896, is so far known by 18 species from China (Guangxi, Yunnan, and Tibet), Myanmar, and northeastern India (*cf.* Ng *et al.*, 2008; 2020; Naruse *et al.*, 2018; Mitra and Waikhom, 2019). *Potamiscus*, however, contains different assemblages of species because each group shows contrasting characters with regard to the carapace, ambulatory legs, male pleon, male telson, male gonopods, and female vulvae; and the genus is almost certainly polyphyletic (Darren C.J. Yeo, unpublished data). Molecular studies on some of the species have already challenged the monophyly of *Potamiscus* (*cf.* Shih *et al.*, 2009; Chu *et al.*, 2017; Zhang

Corresponding Author
Sameer Kumar Pati
sameer_pati@yahoo.co.in

SUBMITTED 13 December 2019
ACCEPTED 29 September 2020
PUBLISHED 05 March 2021

DOI 10.1590/2358-2936e2021006

et al., 2020). Although the genus needs a taxonomic revision involving morphological and molecular data, two new species are described herein from Nagaland State of northeastern India and tentatively assigned to *Potamiscus*: *Potamiscus chizami* sp. nov. and *Potamiscus mima* sp. nov.

India is now known to have 35 genera and 127 species of freshwater crabs, including the two new species described in the present study (*cf.* Mitra *et al.*, 2018; Pati and Thackeray, 2018; Mitra, 2019; Mitra and Waikhom, 2019; Pati *et al.*, 2019a; 2019b; 2020). Among these, 11 genera and 38 species are potamid crabs (*cf.* Mitra *et al.*, 2018; Pati and Thackeray, 2018; Mitra, 2019; Mitra and Waikhom, 2019; Pati *et al.*, 2019a; 2020; present study). Currently, 20 species are known in *Potamiscus*, including seven from India (*cf.* Ng *et al.*, 2008; 2020; Naruse *et al.*, 2018; Mitra and Waikhom, 2019).

Material and Methods

The material examined is deposited in the Zoological Survey of India, Western Regional Centre, Pune, India (ZSI-WRC). The comparative material is from the Crustacea Section, Zoological Survey of India, Kolkata, India (ZSIK).

The terminology is after Ng (1988), with various changes as suggested in Davie *et al.* (2015). The measurement methods of the carapace (in mm) follow Ng (1988). The original camera lucida drawings of the male gonopods were digitally traced using the GNU Image Manipulation Program (GIMP) software by following the suggestions of Montesanto (2015; 2016). The final illustrations were produced after creating stippling effect using the Adobe® Photoshop® software as recommended by Coleman (2018).

The following abbreviations are used: CW, carapace width; CL, carapace length; CH, carapace height; FW, frontal width; a.s.l., above sea level; coll., collected by; P2–P5, pereiopods 2 to 5, respectively; S1–S8, thoracic sternites 1 to 8, respectively; G1, male first gonopod; G2, male second gonopod; VD, minimum distance between female vulvae (Fig. 1); SW, maximum width of sternum (Fig. 1).

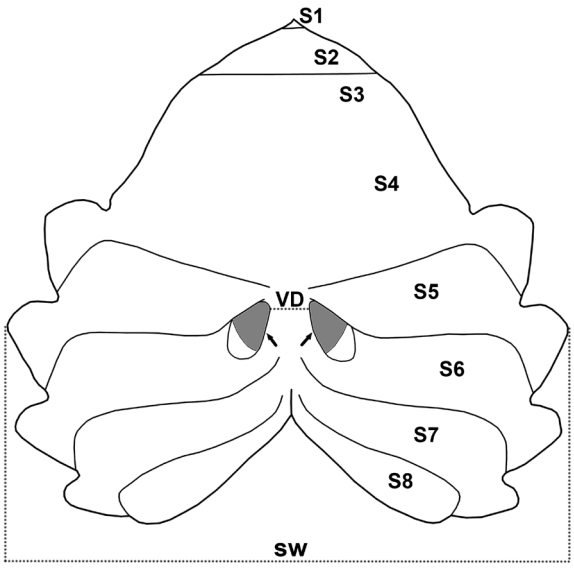

Figure 1. A schematic diagram of female sternum showing measurements. S1–S8, thoracic sternites 1 to 8, respectively; SW, maximum width of sternum; VD, minimum distance between vulvae. Vulvae indicated by arrow marks.

Systematics

Superfamily Potamoidea Ortmann, 1896

Family Potamidae Ortmann, 1896

Subfamily Potamiscinae Bott, 1970 (sensu Yeo and Ng, 2004)

Genus *Potamiscus* Alcock, 1909

Type species. *Potamon* (*Potamiscus*) *annandali* Alcock, 1909, by original designation; gender masculine.

Remarks. *Potamiscus* is so far known by 18 species from China (Guangxi, Yunnan, and Tibet), Myanmar, and northeastern India: *Potamiscus annandali* (Alcock, 1909) (type species); *Potamiscus cangyuanensis* Dai, 1999; *Potamiscus crassus* Naruse, Chia and Zhou, 2018; *Potamiscus decourcyi* (Kemp, 1913); *Potamiscus elaphrius* Dai, Chen, Liu, Luo, Yi, Liu, Gu and Liu, 1990; *Potamiscus fumariatus* Naruse, Chia and Zhou, 2018; *Potamiscus loshingensis* (Wu, 1934); *Potamiscus montosus* Tai, Song, He, Cao, Xu and Zhong, 1975; *Potamiscus*

motuoensis Dai, 1990; *Potamiscus palelensis* Mitra and Waikhom, 2019; *Potamiscus pealianus* (Wood-Mason, 1871); *Potamiscus rangoonensis* (Rathbun, 1904); *Potamiscus rongjingensis* Dai, Chen, Liu, Luo, Yi, Liu, Gu and Liu, 1990; *Potamiscus tumidulus* (Alcock, 1909); *Potamiscus whitteni* Ng, Hla Htoo and Win Mar, 2020; *Potamiscus yiwuensis* Dai and Cai, 1998; *Potamiscus yongshengensis* Dai and Chen, 1985; and *Potamiscus yunnanensis* (Kemp, 1923) (Ng *et al.*, 2008; 2020; Naruse *et al.*, 2018; Mitra and Waikhom, 2019).

While the monophyly of *Potamiscus* was previously challenged (*cf.* Shih *et al.*, 2009; Chu *et al.*, 2017; Zhang *et al.*, 2020), the genus is currently defined morphologically by its moderately high carapace with a rugose dorsal surface, completely absent or vestigial flagellum on the third maxilliped exopod, subconical G1 with distally tapering tip, absence of a dorsal flap on the G1 terminal segment, and marginal position of the groove for the G2 on the G1 terminal segment (*cf.* Naruse *et al.*, 2018). The two new species of *Potamiscus* described here generally agree with the present definition of the genus (*sensu* Naruse *et al.*, 2018) except for their distinct, but low, dorsal flap on the G1 terminal segment. The dorsal flap is also distinct in *Po. crassus*, *Po. tumidulus*, and *Po. whitteni* (*cf.* Naruse *et al.*, 2018; Ng *et al.*, 2020; personal observation), whereas it is only slightly developed in *Po. palelensis*, *Po. pealianus*, and *Po. rangoonensis* (*cf.* Bott, 1970; Türkay and Naiyanetr, 1987; Mitra and Waikhom, 2019). The remaining species do not possess a dorsal flap on the G1 terminal segment.

It is worth mentioning that existing and the present new species of *Potamiscus* can be separated into the following distinct groups based on their G1 terminal segment. "Group I" consists of *Po. annandali* (type species), *Po. cangyuanensis*, *Po. decourcyi*, *Po. montosus*, *Po. rangoonensis*, and *Po. yiwuensis*; all have a slender, conical or subconical, and short G1 terminal segment, *i.e.*, approximately 0.2–0.3 times the length of the subterminal segment (*cf.* Bott, 1970; Türkay and Naiyanetr, 1987; Dai and Cai, 1998; Dai, 1999; personal observation). "Group II" comprises *Po. chizami* sp. nov., *Po. mima* sp. nov., *Po. palelensis*, *Po. tumidulus*, and *Po. whitteni*; all share a slender, conical or subconical, and relatively long G1 terminal segment, *i.e.*, approximately 0.4–0.45 times the length of the subterminal segment (*cf.* Mitra and Waikhom, 2019; Ng *et al.*, 2020; present study). *Potamiscus crassus*, *Po. yongshengensis*, and *Po. yunnanensis* constitute "Group III" due to their stout, conical or subconical, and relatively long terminal segment of the G1, which is about 0.5–0.6 times the length of the subterminal segment (*cf.* Dai, 1999; Naruse *et al.*, 2018). The species in "Group IV" possess a stout, cylindrical or subcylindrical, and relatively long G1 terminal segment, measuring about 0.4–0.6 times the length of the subterminal segment and are represented by *Po. elaphrius*, *Po. fumariatus*, *Po. loshingensis*, *Po. motuoensis*, and *Po. rongjingensis* (*cf.* Dai, 1999; Naruse *et al.*, 2018). *Potamiscus pealianus* has a slender, cylindrical, and relatively long G1 terminal segment (*i.e.*, approximately 0.45 times the length of the subterminal segment) (*cf.* Bott, 1970), which seems to be a transitional state to the characters shown by Groups I–IV.

Comparative material. *Potamiscus annandali*: lectotype male (33.0 × 25.0 mm), Nemotha, Cachar district, Assam, India, collection date unknown, coll. J. Wood-Mason (ZSIK 6602-3/9). *Potamiscus decourcyi*: holotype male (63.0 × 49.0 mm), Sirpo Valley, near Renging, East Siang district, Arunachal Pradesh, India, March 1912, coll. M.W.R. de Courcy (ZSIK 8006/10). *Potamiscus palelensis*: holotype male (29.5 × 24.2 mm), Palel, Kakching district, Manipur, India, 24 September 2017, coll. M.D. Waikhom (ZSIK C.6466/2). *Potamiscus tumidulus*: syntype male (17.9 × 14.7 mm), Sikkim, India, collection date unknown, coll. J. Wood-Mason (ZSIK 5507/10).

***Potamiscus chizami* sp. nov.**

(Figs. 2A–F, 3A–D, 4A–C)

Zoobank: urn:lsid:zoobank.org:act:0EB4C575-8D19-4025-B80F-94973E782B48

Type material. Holotype: adult male (CW 31.22 mm, CL 24.19 mm, CH 17.97 mm, FW 8.63 mm), Chizami, Phek District, Nagaland, India (25.600°N 94.394°E), altitude 1424 m a.s.l., 8 July 2017, coll. Rukuto (ZSI-WRC C.1950). Paratypes: adult male (CW 29.10 mm, CL 22.67 mm, CH 16.82 mm, FW 8.96 mm) and adult female (CW 27.71 mm, CL 21.26 mm, CH 16.01 mm, FW 8.21 mm), same data as holotype (ZSI-WRC C.1951); adult male (CW 27.71 mm, CL 21.35 mm, CH 15.68 mm, FW 8.00 mm) and adult female (CW 27.81 mm, CL 21.27 mm, CH 16.29 mm, FW 8.20 mm), same data as holotype (ZSI-WRC C.1952).

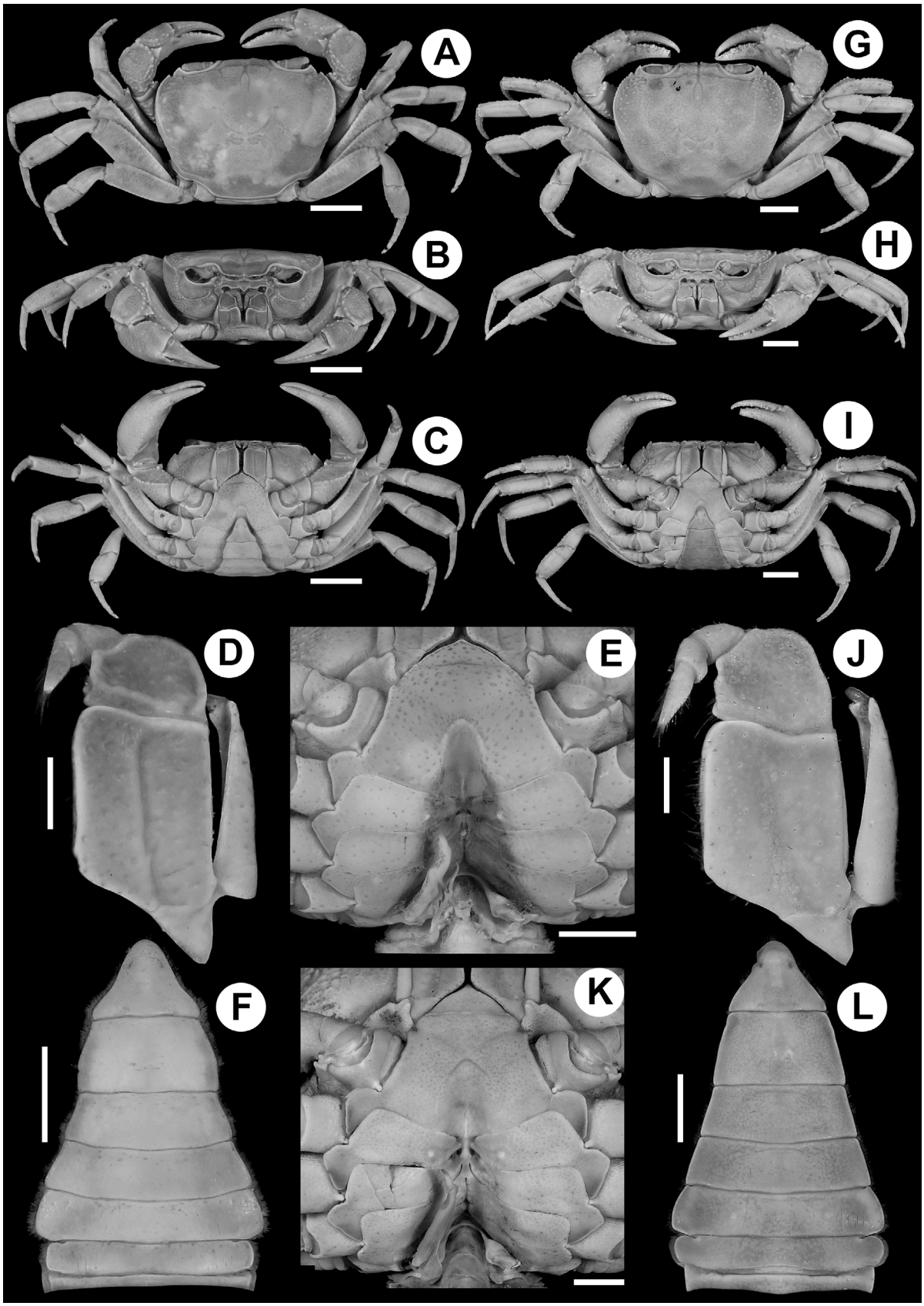

Figure 2. *Potamiscus chizami* sp. nov., holotype male (31.22 × 24.19 mm) (ZSI-WRC C.1950) (**A–F**); *Potamiscus mima* sp. nov., holotype male (42.65 × 33.82 mm) (ZSI-WRC C.1954) (**G–L**). **A, G**, overall dorsal view; **B, H**, overall frontal view; **C, I**, overall ventral view; **D, J**, left third maxilliped; **E, K**, thoracic sternites with G1 *in situ* (left G1 removed); **F, L**, pleonal somites 1–6 and telson. Scale bars = 10 mm (**A–C, G–I**), 5 mm (**E, F, K, L**), 2 mm (**D, J**).

Additional material. 2 males (CW 27.89–28.35 mm, CL 21.45–21.93 mm, CH 15.92–15.97 mm, FW 8.37–8.57 mm) and 3 females (CW 24.75–25.90 mm, CL 18.96–19.82 mm, CH 14.10–14.52 mm, FW 7.61–7.84 mm), same data as holotype (ZSI-WRC C.1953).

Diagnosis. Carapace small (CW < 32 mm), subovate, broad (CW/CL = 1.3), deep (CH/CW = 0.6); dorsal surface convex in frontal view; anterolateral margins cristate; frontal margin broad (FW/CW = 0.3); epigastric cristae distinct, anterior to postorbital cristae, separated from latter by long, distinct groove; postorbital cristae distinct, sharp, not confluent with epibranchial tooth; external orbital angle triangular, with relatively short outer margin, approximately 1.5 times length of inner margin; epibranchial tooth distinct, with distinct cleft; cervical grooves indiscernible; suborbital margin confluent with supraorbital margin (Figs. 2A–C, 4A, B). Third maxilliped exopod with vestigial flagellum (Fig. 2D). Chelipeds generally smooth, asymmetrical, with broad inner distal major tooth on carpus (Figs. 2A–C, 4A, B). Ambulatory legs relatively stout (P3 merus approximately 3.0 times long as broad), short, generally glabrous (Figs. 2A–C, 4A, B). Suture between male S2/S3 distinct as moderately deep, narrow groove, reaching lateral margins; suture between male S3/S4 indiscernible (Fig. 2C, E). Male sternopleonal cavity relatively long, reaching to imaginary line joining medial part of cheliped coxae (Fig. 2C, E). Male pleon broad, triangular, with strongly concave lateral margins; somites 1, 2 equally broad; somite 6 trapezoidal, distinctly broad, with convex lateral margins (Fig. 2C, F). Male telson as long as pleonal somite 6, with strongly concave lateral margins (Fig. 2C, F). G1 relatively slender, with terminal segment bent outwards at angle of about 30° from longitudinal axis, tip narrow, reaching beyond pleonal locking tubercle, not touching suture S4/S5 *in situ*; flexible zone small; terminal segment sinuous, slender, subconical, long, approximately 0.4 times combined length of flexible zone and subterminal segment, distal third narrow, gently curved, dorsal flap distinct but low, broadly rounded; subterminal segment gently sinuous (Figs. 2E, 3A–C). G2 distinctly longer than G1, approximately 1.3 times length of G1; distal segment long, approximately 0.7 times length of basal segment (Fig. 3C, D). Vulvae on S6 relatively closely located, suborbicular, large, occupying two-thirds length of S6, anterior margin touching suture S5/S6 with mesial end clearly away from suture S4/S5 (Fig. 4C).

Description of male holotype. Carapace transversely subovate, broader than long (CW/CL = 1.3), deep (CH/CW = 0.6); dorsal surface convex in frontal view, glabrous, smooth except for epigastric cristae, postorbital cristae and epibranchial region; anterolateral surface gently inflated in frontal view; anterolateral margins convex, granular, distinctly emarginated at distal quarter, raised, separated from anterolateral surface by shallow groove; posterolateral margins converging posteriorly, joining with gently concave posterior margin; front trapezoidal, anterior portion strongly deflexed; frontal margin gently concave medially, broad (FW/CW = 0.3); epigastric cristae distinct, generally smooth, anterior to postorbital cristae, separated from latter by long, distinct groove; postorbital cristae distinct, sharp, not confluent with epibranchial tooth; external orbital angle triangular, with gently convex, short outer margin, approximately 1.5 times length of inner margin; epibranchial tooth low, blunt, positioned above level of postorbital cristae, cleft distinct; postorbital region concave; branchial regions inflated, smooth except for strongly granular epibranchial region; cervical grooves barely visible; mesogastric groove deep, narrow, long, extending into frontal region, bifurcated posteriorly; H-shaped groove visible; subhepatic region rugose; suborbital region generally smooth, glabrous; suborbital margin concave, cristate, smooth, joining with supraorbital margin; pterygostomial region smooth except for anteriorly located low granules; frontal medial triangle incomplete, with dorsal margin only, lateral margins indiscernible; epistome posterior margin with distinct, triangular medial tooth and strongly sinuous lateral margins (Fig. 2A–C).

Eyes smaller than orbital space; eye stalk short, narrow; cornea large, pigmented (Fig. 2B).

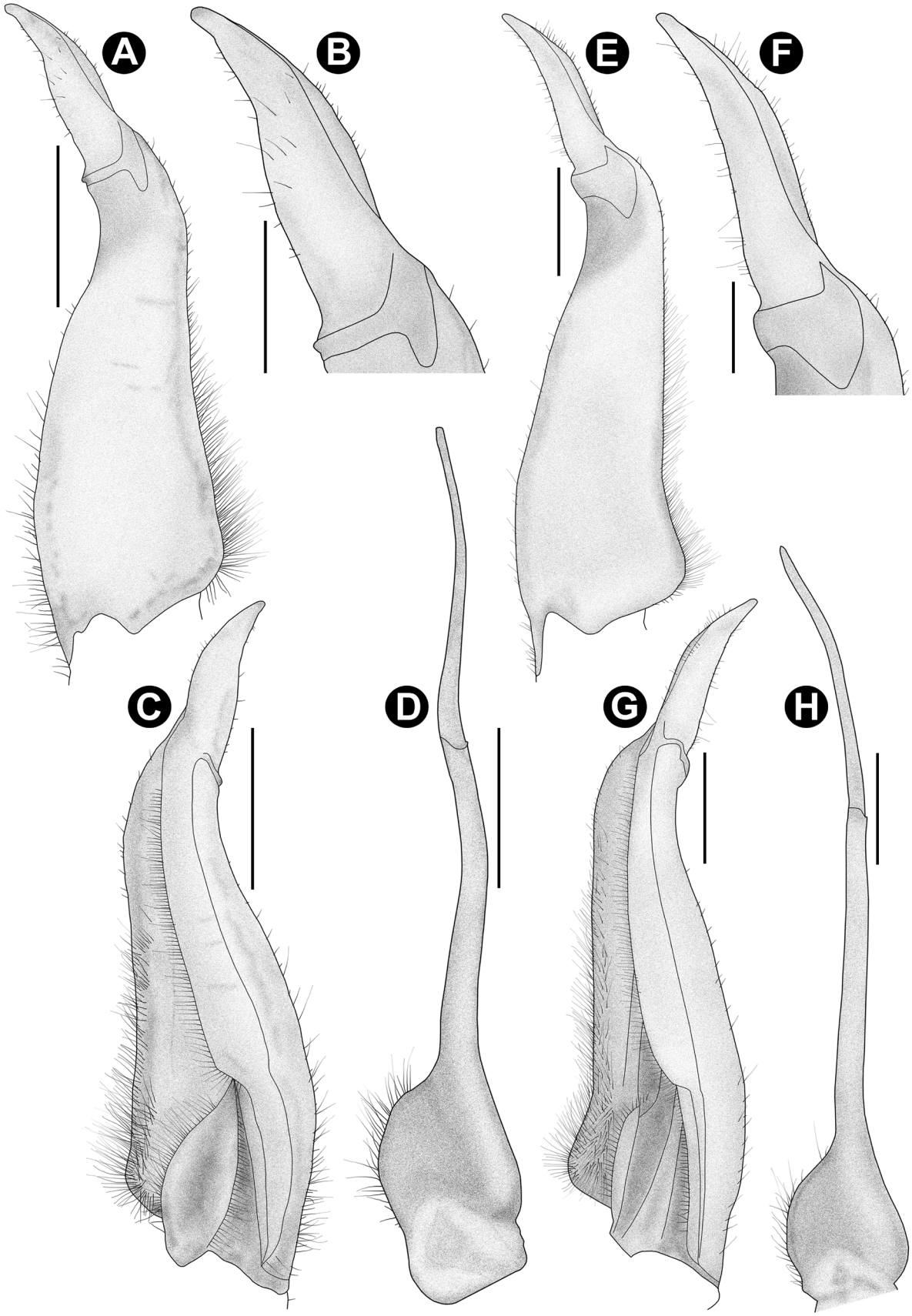

Figure 3. *Potamiscus chizami* sp. nov., holotype male (31.22 × 24.19 mm) (ZSI-WRC C.1950) (**A–D**); *Potamiscus mima* sp. nov., holotype male (42.65 × 33.82 mm) (ZSI-WRC C.1954) (**E–H**). **A, E**, dorsal view of left G1; **B, F**, dorsal view of left G1 terminal segment; **C, G**, ventral view of left G1; **D, H**, left G2. Scale bars = 2 mm (**A, C–E, G, H**), 1 mm (**B, F**).

Antennules long, folded in longitudinally broad fossae; antennae very short, reaching slightly beyond base of eye stalk (Fig. 2B). Mandibular palp 3-segmented; terminal segment simple, undivided. First, second maxillipeds each with long flagellum on exopod. Third maxillipeds cover most of buccal cavity when closed; ischium subrectangular, longer than broad, with narrow, deep, oblique medial groove; merus subpentagonal, broader than long, depressed; exopod slender, distally narrow, longer than ischium, reaching proximal third of merus, with vestigial flagellum, approximately 0.25 times merus width (Fig. 2B–D).

Chelipeds generally smooth, asymmetrical, right chela larger (Fig. 2A–C). Major chela with 3 or 4 large, blunt teeth on each finger, small gape when fingers closed; dactylus smooth, gently curved, slender, longer than upper margin of palm, proximally with 4 distinct to low dorsal granules; palm slightly longer than high, with widely spaced, distinct but low granules on upper- and lower surfaces; carpus slightly rugose, gently inflated, with stout, sharp, triangular inner distal major tooth and low, moderately sharp subbasal tooth; merus rugose on outer surface, lacking subterminal spine (Fig. 2A–C).

Ambulatory legs moderately stout (P3 merus approximately 3 times long as broad), short, P3 longest, generally glabrous; merus (P2–P5) long, lacking subdistal spine; propodus (P2–P5) moderately stout; dactylus (P2–P5) gently recurved, slightly longer than propodus, with short, sharp chitinous spines on margins (Fig. 2A–C).

Thoracic sternites punctate, glabrous; S1 and S2 completely fused; suture S2/S3 distinct as moderately deep, narrow groove, reaching lateral margins; suture S3/S4 indiscernible; suture S4/S5, S5/S6, S6/S7 shallow, narrow, medially indiscernible; suture S7/S8 laterally indiscernible, only visible towards sternopleonal cavity but interrupted by longitudinal groove between S7 and S8, lacking transverse ridge (Fig. 2C, E). Pleonal locking mechanism with prominent tubercle on submedial part of S5 (Fig. 2E). Sternopleonal cavity deep, long, reaching to imaginary line joining medial part of cheliped coxae (Fig. 2C, E).

Pleon broad, triangular, with strongly concave lateral margins; somites 1, 2 almost rectangular, narrower than somite 3; somites 3–5 trapezoidal, with distally converging lateral margins; somite 6 trapezoidal, broader than long (proximal width approximately 1.8 times medial length), distinctly longer than preceding somites, equal in length to telson, with convex lateral margins (Fig. 2C, F). Telson triangular, broader than long (proximal width approximately 1.4 times medial length), with strongly concave lateral margins, apex narrow, round (Fig. 2C, F).

G1 moderately stout, with terminal segment bent outwards at angle of about 30° from longitudinal axis, tip narrow, reaching beyond pleonal locking tubercle, not touching suture S4/S5 *in situ*; flexible zone small; terminal segment sinuous, slender, subconical, long, approximately 0.4 times combined length of flexible zone and subterminal segment, distal third narrow, gently curved, dorsal flap distinct but low, broadly rounded; subterminal segment gently sinuous, distal third narrow, broad at base (Figs. 2E, 3A–C). G2 distinctly longer than G1, approximately 1.3 times length of G1; distal segment sinuous, subcylindrical, long, approximately 0.7 times length of basal segment; basal segment stout at proximal third, appearing ovate (Fig. 3C, D).

Paratypes. The male paratypes (ZSI-WRC C.1951, 1952) resemble the holotype in all the carapace and gonopod features. The female paratypes (ZSI-WRC C.1951, 1952) also share most of the non-sexual character states with the holotype. The pleon of the female paratypes is narrowly ovate, which covers the thoracic sternum except for S1, S2, and lateral edges when closed (Fig. 4B). In the female paratypes, pleonal somite 1 is the shortest; pleonal somites 2–5 are progressively longer; and pleonal somite 6 is the longest, much broader than long, almost equal in length to the telson, with gently convex lateral margins (Fig. 4B). The female telson is broadly ovate, much broader than long, with gently convex lateral margins and round apex (Fig. 4B). The vulvae on S6 are close to each other (VD/SW = approximately 0.1), suborbicular, open laterally, large, occupying two-thirds the length of S6, deep, anterior margin touching the suture S5/S6 with the mesial end clearly away from the suture S4/S5, and laterally partially covered by a protruding sternal cover (Fig. 4C).

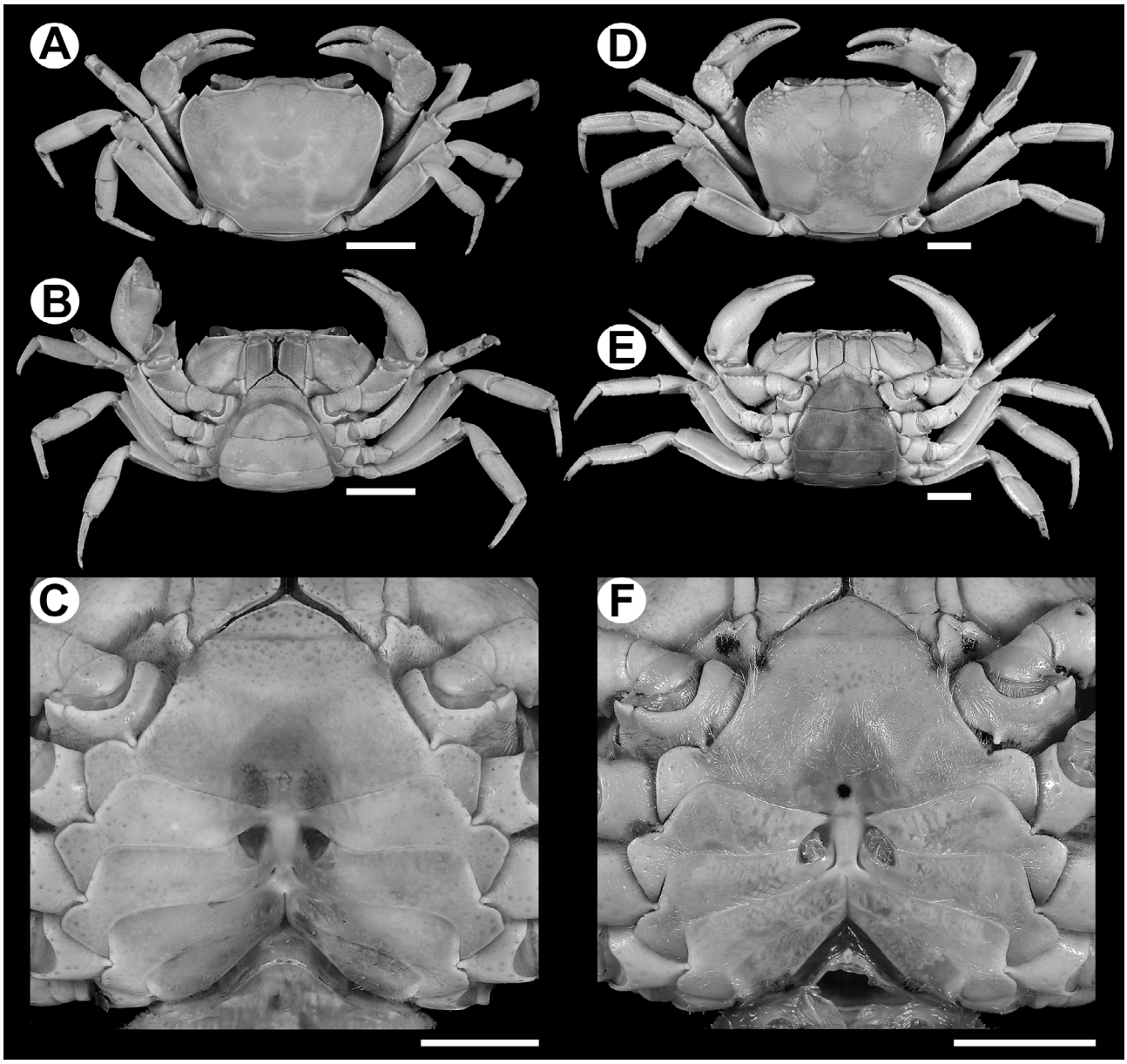

Figure 4. *Potamiscus chizami* sp. nov., paratype female (27.71 × 21.26 mm) (ZSI-WRC C.1951) (**A–C**); *Potamiscus mima* sp. nov., paratype female (43.04 × 33.27 mm) (ZSI-WRC C.1955) (**D–F**). **A, D**, overall dorsal view; **B, E**, overall ventral view; **C, F**, thoracic sternites showing vulvae. Scale bars = 10 mm (**A, B, D–F**), 5 mm (**C**).

Etymology. The species is named after the type locality, Chizami, a large village in the Phek District of Nagaland State, India. Used as a noun in apposition.

Remarks. *Potamiscus chizami* sp. nov. most resembles three Indian species (*Po. mima* sp. nov., *Po. palelensis*, and *Po. tumidulus*) and a species from Myanmar (*Po. whitteni*) than any other congeners due to its slender, subconical, sinuous, gently outwardly curved, and long G1 terminal segment (approximately 0.4 times the combined length of the flexible zone and subterminal segment), with a distinct but low dorsal flap (Fig. 3A–C, E–G; *cf.* Mitra and Waikhom, 2019: figs. 2A, B, E, F, 4A–C for *Po. palelensis*; Ng *et al.*, 2020: fig. 3D for *Po. whitteni*; personal observation for *Po. tumidulus*). Although these five species have a similar looking G1 terminal segment, *Po. chizami* sp. nov., *Po. mima* sp. nov., *Po. palelensis*, and *Po. whitteni* can still be differentiated from *Po. tumidulus* due to their relatively slender G1 (Fig. 3A, C, E, G; *cf.* Mitra and Waikhom, 2019: figs. 2A, E, 4A, B; Ng *et al.*, 2020: fig. 3D) against the relatively stout G1 of *Po. tumidulus* (personal observation). Furthermore, the G1 tip reaches the pleonal locking tubercle in

Po. chizami sp. nov. and *Po. mima* sp. nov. (Fig. 2E, K), whereas it never reaches the pleonal locking tubercle in *Po. tumidulus* (personal observation).

In carapace morphology, *Po. chizami* sp. nov., *Po. mima* sp. nov., *Po. palelensis*, and *Po. whitteni* are very distinct from *Po. tumidulus* in the following characters: the postorbital crista is relatively sharp (Figs. 2A, G, 4A, D; *cf.* Mitra and Waikhom, 2019: fig. 1A; Ng *et al.*, 2020: fig. 1A–C) (*vs.* rugose postorbital crista in *Po. tumidulus*; personal observation); the external orbital angle is triangular, with short outer margin, approximately 1–2 times the length of the inner margin (Figs. 2A, G, 4A, D; *cf.* Mitra and Waikhom, 2019: fig. 1A; Ng *et al.*, 2020: fig. 1A–C) (*vs.* broadly triangular external orbital angle, with long outer margin, approximately 3 times the length of the inner margin in *Po. tumidulus*; personal observation); the epibranchial tooth is distinct, with the cleft separating it from the external orbital angle being distinct (Figs. 2A, G, 4A, D; *cf.* Mitra and Waikhom, 2019: fig. 1A; Ng *et al.*, 2020: fig. 1A–C) (*vs.* indistinct epibranchial tooth and cleft in *Po. tumidulus*; personal observation); the suture between male S3/S4 is either indiscernible or only visible as a shallow depression (Fig. 2C, E, I, K; *cf.* Mitra and Waikhom, 2019: fig. 1C; Ng *et al.*, 2020: fig. 2A, B) (*vs.* distinct and deep suture between male S3/S4 in *Po. tumidulus*; personal observation); and the male sternopleonal cavity is relatively long, reaching to the imaginary line joining the medial part of the cheliped coxae (Fig. 2C, E, I, K; *cf.* Mitra and Waikhom, 2019: fig. 1C; Ng *et al.*, 2020: fig. 2A, B) (*vs.* relatively short male sternopleonal cavity, reaching only to the imaginary line joining the posterior part of the cheliped coxae in *Po. tumidulus*; personal observation).

Although *Po. chizami* sp. nov. is similar to *Po. palelensis* in carapace morphology and G1 structure, it is nevertheless distinguished from *Po. palelensis* mainly by its indiscernible cervical grooves (Figs. 2A, 4A) (*vs.* relatively distinct cervical grooves; *cf.* Mitra and Waikhom, 2019: fig. 1A), the relatively stout ambulatory legs, P3 merus approximately 3.0 times long as broad (Figs. 2A, 4A) (*vs.* relatively slender ambulatory legs, P3 merus approximately 3.7 times long as broad; *cf.* Mitra and Waikhom, 2019: fig. 1A), the gently curved distal third of the G1 terminal segment (Fig. 3A, B) (*vs.* distinctly curved distal third of the G1 terminal segment; *cf.* Mitra and Waikhom, 2019: figs. 2A, B, 4A, C), and the relatively stouter G1 subterminal segment (Fig. 3A) (*vs.* relatively slender G1 subterminal segment; *cf.* Mitra and Waikhom, 2019: figs. 2A, 4A).

The similarities in carapace and G1 structures notwithstanding, *Po. chizami* sp. nov. is distinguished from *Po. mima* sp. nov. by its distinctly convex dorsal surface of the carapace (Fig. 2B) [*vs.* gently convex dorsal surface (Fig. 2H)], the distinct groove between epigastric- and postorbital cristae (Figs. 2A, 4A) [*vs.* barely visible groove between epigastric- and postorbital cristae (Figs. 2G, 4D)], the confluent suborbital- and supraorbital margins (Fig. 2B) [*vs.* separation of the suborbital margin from the supraorbital margin by the external orbital angle (Fig. 2H)], the relatively broad male pleon with the strongly concave lateral margins (Fig. 2C, F) [*vs.* relatively narrow male pleon with the gently concave lateral margins (Fig. 2I, L)], equally broad male pleonal somites 1, 2 (Fig. 2F) [*vs.* broader male pleonal somite 2 than somite 1 (Fig. 2L)], the convex lateral margins of the male pleonal somite 6 (Fig. 2C, F) [*vs.* straight lateral margins (Fig. 2I, L)], the smaller flexible zone on G1 (Fig. 3A, B) [*vs.* larger flexible zone on G1 (Fig. 3E, F)], the relatively more stout G1 terminal segment (Fig. 3A–C) [*vs.* relatively slender G1 terminal segment (Fig. 3E–G)], the relatively longer G2, approximately 1.3 times the G1 length (Fig. 3C, D) [*vs.* relatively shorter G2, approximately 1.1 times the G1 length (Fig. 3G, H)], and the suborbicular vulvae, with the mesial end of the vulval anterior margin clearly away from the suture S4/S5 (Fig. 4C) [*vs.* ovate vulvae, with the mesial end of the vulval anterior margin reaching close to the suture S4/S5 (Fig. 4F)]. Moreover, on the basis of the material available, adult *Po. chizami* sp. nov. appears to be a smaller species (CW < 32 mm) than *Po. mima* sp. nov. (CW < 53 mm).

Although *Po. chizami* sp. nov. shares many features of the carapace and G1 with the congener from Myanmar, *Po. whitteni*, the new species is easily separated from *Po. whitteni* by its indiscernible cervical grooves (Figs. 2A, 4A) (*vs.* relatively distinct cervical grooves; *cf.* Ng *et al.*, 2020: fig. 1A–C), the strongly convex lateral margins of the male pleonal somite 6 (Fig. 2C, F) (*vs.* gently convex lateral margins of the male pleonal somite 6; *cf.* Ng *et al.*, 2020: figs. 2A,

B, 3A), the strongly concave lateral margins of the male telson (Fig. 2C, F) (*vs.* gently concave to almost straight lateral margins of the male telson; *cf.* Ng *et al.*, 2020: figs. 2A, B, 3A), and the relatively stouter G1 terminal segment, with straight tip (Fig. 3A–C) (*vs.* relatively slender G1 terminal segment, with upcurved tip; *cf.* Ng *et al.*, 2020: fig. 3C–F).

Geographical distribution. *Potamiscus chizami* sp. nov. is known only from Chizami village in Phek District of Nagaland, northeastern India.

***Potamiscus mima* sp. nov.**

(Figs. 2G–L, 3E–H, 4D–F)

Zoobank: urn:lsid:zoobank.org:act:F2462728-23EC-448E-AAF5-E64286258BCD

Type material. Holotype: adult male (CW 42.65 mm, CL 33.82 mm, CH 22.16 mm, FW 9.83 mm), Mima, Kohima District, Nagaland, India (25.591°N 94.110°E), altitude 2105 m a.s.l., 6 July 2017, coll. Apeyo (ZSI-WRC C.1954). Paratypes: adult male (CW 44.94 mm, CL 34.27 mm, CH 23.29 mm, FW 11.08 mm) and adult female (CW 43.04 mm, CL 33.27 mm, CH 22.98 mm, FW 10.57 mm), same data as holotype (ZSI-WRC C.1955); adult male (CW 38.87 mm, CL 31.01 mm, CH 20.91 mm, FW 10.11 mm) and adult female (CW 41.51 mm, CL 31.57 mm, CH 22.55 mm, FW 10.46 mm), same data as holotype (ZSI-WRC C.1956).

Additional material. 6 males (CW 39.60–52.50 mm, CL 31.37–40.61 mm, CH 20.76–26.59 mm, FW 10.22–12.18 mm), same data as holotype (ZSI-WRC C.1957); 7 females (CW 35.41–44.11 mm, CL 28.06–34.40 mm, CH 19.77–24.07 mm, FW 8.92–11.23 mm), same data as holotype (ZSI-WRC C.1958).

Diagnosis. Carapace large (CW < 53 mm), subovate, broad (CW/CL = 1.3), moderately deep (CH/CW = 0.5–0.6); dorsal surface gently convex in frontal view; anterolateral margins cristate; frontal margin narrow (FW/CW = 0.25); epigastric cristae distinct, slightly anterior to postorbital cristae, groove separating it from latter barely visible; postorbital cristae distinct, sharp, not confluent with epibranchial tooth; external orbital angle triangular, with relatively short outer margin, subequal in length to inner margin; epibranchial tooth distinct, with distinct cleft; cervical grooves indiscernible; suborbital margin separated from supraorbital margin by external orbital angle (Figs. 2G–I, 4D, E). Third maxilliped exopod with vestigial flagellum (Fig. 2J). Chelipeds rugose, asymmetrical, with broad inner distal major tooth on carpus (Figs. 2G–I, 4D, E). Ambulatory legs relatively stout (P3 merus approximately 2.8 times long as broad), short, generally glabrous (Figs. 2G–I, 4D, E). Suture between male S2/S3 distinct as shallow, narrow groove, reaching lateral margins; suture between male S3/S4 visible as shallow depression, running from edge of sternopleonal cavity to lateral margins (Fig. 2I, K). Male sternopleonal cavity relatively long, reaching to imaginary line joining medial part of cheliped coxae (Fig. 2I, K). Male pleon narrow, triangular, with gently concave lateral margins; somite 2 broader than somite 1; somite 6 trapezoidal, distinctly broad, with straight lateral margins (Fig. 2I, L). Male telson as long as pleonal somite 6, with strongly concave lateral margins (Fig. 2I, L). G1 relatively slender, with terminal segment bent outwards at angle of about 30° from longitudinal axis, tip narrow, reaching to pleonal locking tubercle or beyond, not touching suture S4/S5 *in situ*; flexible zone large; terminal segment sinuous, slender, subconical, long, approximately 0.4 times combined length of flexible zone and subterminal segment, distal third gently curved, dorsal flap distinct but low, broadly rounded; subterminal segment sinuous (Figs. 2K, 3E–G). G2 slightly longer than G1, approximately 1.1 times length of G1; distal segment long, approximately 0.6 times length of basal segment (Fig. 3G, H). Vulvae on S6 relatively closely located, ovate, large, occupying two-thirds length of S6, anterior margin touching suture S5/S6 with mesial end reaching close to suture S4/S5 (Fig. 4F).

Description of male holotype. Carapace transversely subovate, broader than long (CW/CL = 1.3), moderately deep (CH/CW = 0.5); dorsal surface gently convex in frontal view, glabrous, smooth except for frontal region, epigastric cristae, postorbital cristae, branchial regions and posterolateral margins; anterolateral surface gently inflated in frontal view; anterolateral margins convex, granular, distinctly emarginated at distal quarter, raised, separated from anterolateral surface by distinct groove; posterolateral margins rugose,

converging posteriorly, joining with gently concave posterior margin; front trapezoidal, anterior portion strongly deflexed, divided into 2 rectangular, rugose lobes; frontal margin concave medially, narrow (FW/CW = 0.25); epigastric cristae distinct, rugose, slightly anterior to postorbital cristae, groove separating it from latter barely visible; postorbital cristae distinct, sharp, not confluent with epibranchial tooth; external orbital angle triangular, with gently convex, short outer margin, subequal in length to inner margin; epibranchial tooth distinct, blunt, positioned above level of postorbital cristae, cleft distinct; postorbital region concave; branchial regions gently inflated, strongly granular anterolaterally; cervical grooves barely visible; mesogastric groove deep, narrow, long, extending into frontal region, bifurcated posteriorly; H-shaped groove visible; subhepatic region highly rugose; suborbital region smooth except for few low granules, glabrous; suborbital margin concave, cristate, with few very low granules, not joining with supraorbital margin; pterygostomial region smooth except for anteriorly located low granules; frontal medial triangle incomplete, with dorsal margin only, lateral margins indiscernible; epistome posterior margin with well-developed, triangular medial tooth, outer parts sloping downwards laterally (Fig. 2G–I).

Eyes smaller than orbital space; eye stalk short, narrow; cornea moderately large, pigmented (Fig. 2H).

Antennules long, folded in longitudinally narrow fossae; antennae very short, reaching slightly beyond base of eye stalk (Fig. 2H). Mandibular palp 3-segmented; terminal segment simple, undivided. First, second maxillipeds each with long flagellum on exopod. Third maxillipeds cover most of buccal cavity when closed; ischium subrectangular, longer than broad, with broad, moderately deep, oblique medial groove; merus subpentagonal, broader than long, depressed; exopod slender, distally narrow, longer than ischium, reaching proximal quarter of merus, with vestigial flagellum, approximately 0.2 times merus width (Fig. 2H–J).

Chelipeds rugose, asymmetrical, right chela larger (Fig. 2G–I). Major chela with 4 or 5 large, blunt teeth on each finger, small gape when fingers closed; dactylus slightly rugose, gently curved, moderately stout, longer than upper margin of palm, with 3 or 4 distinct but low dorsal granules on proximal third; palm slightly longer than high, with widely spaced, distinct granules on outer-, upper- and lower surfaces; carpus rugose, sunken anteromedially, with stout, sharp, triangular inner distal major tooth and low, moderately sharp sub-basal tooth; merus rugose on outer surface, lacking subterminal spine (Fig. 2G–I).

Ambulatory legs moderately stout (P3 merus approximately 2.8 times long as broad), short, P3 longest, generally glabrous; merus (P2–P5) elongate, lacking subdistal spine; propodus (P2–P5) moderately stout; dactylus (P2–P5) gently recurved, slightly longer than propodus, with short, sharp chitinous spines on margins (Fig. 2G–I).

Thoracic sternites generally smooth and glabrous; S1 and S2 completely fused; suture S2/S3 distinct as shallow, narrow groove, reaching lateral margins; suture S3/S4 visible as very shallow depression, running from edge of sternopleonal cavity to lateral margins; suture S4/S5, S5/S6, S6/S7 shallow, narrow, medially indiscernible; suture S7/S8 laterally indiscernible, only visible towards sternopleonal cavity but interrupted by longitudinal groove between S7 and S8, lacking transverse ridge (Fig. 2I, K). Pleonal locking mechanism with prominent tubercle on submedial part of S5 (Fig. 2K). Sternopleonal cavity deep, long, reaching to imaginary line joining medial part of cheliped coxae (Fig. 2I, K).

Pleon narrow, triangular, with gently concave lateral margins; somite 1 rectangular, narrower than somite 2; somite 2 almost rectangular, with strongly convex lateral margins; somites 3–5 trapezoidal, with converging lateral margins; somite 6 trapezoidal, broader than long (proximal width approximately 1.8 times medial length), distinctly longer than preceding somites, almost equal in length to telson, with straight lateral margins (Fig. 2I, L). Telson triangular, broader than long (proximal width approximately 1.4 times medial length), with strongly concave lateral margins, apex narrow, round (Fig. 2I, L).

G1 moderately stout, with terminal segment bent outwards at angle of about 30° from longitudinal axis, tip narrow, reaching to pleonal locking tubercle *in situ*; flexible zone large; terminal segment sinuous, slender, subconical, long, approximately 0.4 times combined length of flexible zone and subterminal segment, distal third gently curved, dorsal flap distinct but low, broadly rounded; subterminal segment sinuous, distal

quarter narrow, broad at base (Figs. 2K, 3E–G). G2 slightly longer than G1, approximately 1.1 times length of G1; distal segment gently curved, subcylindrical, long, approximately 0.6 times length of basal segment; basal segment stout at proximal third, appearing ovate (Fig. 3G, H).

Paratypes. The male paratypes (ZSI-WRC C.1955, 1956) are similar to the holotype in both external morphology and gonopod structure. The only exception is the G1 tip of the smaller male paratype (ZSI-WRC C.1956) that reaches beyond the pleonal locking tubercle, but never touches suture S4/S5. The G1 tip only reaches to the pleonal locking tubercle in the holotype and the larger male paratype. The female paratypes (ZSI-WRC C.1955, 1956) have no differences in non-sexual character states with the holotype. The female paratypes have a narrowly ovate pleon that covers the thoracic sternum except for S1, S2, and lateral edges when closed (Fig. 4E). In the female paratypes, pleonal somite 1 is the shortest; pleonal somites 2–5 are progressively longer; and pleonal somite 6 is the longest, much broader than long, almost equal in length to the telson, with convex lateral margins (Fig. 4E). The female telson is broadly ovate, much broader than long, with convex lateral margins and round apex (Fig. 4E). The vulvae on S6 are close to each other (VD/SW = approximately 0.1), ovate, large, occupying two-thirds the length of S6, deep, anterior margin touching the suture S5/S6 with the mesial end reaching close to the suture S4/S5, and completely covered by a soft operculum (Fig. 4F).

Etymology. The species is named after the type locality, Mima, a large village in the Kohima District of Nagaland State, India. Used as a noun in apposition.

Remarks. *Potamiscus mima* sp. nov. is strikingly similar to three Indian congeners (*Po. chizami* sp. nov., *Po. palelensis*, and *Po. tumidulus*) and a species from Myanmar (*Po. whitteni*) due to the presence of a slender, subconical, sinuous, gently outwardly curved, and relatively long terminal segment of the G1, which measures about 0.4 times the combined length of the flexible zone and subterminal segment and possesses a distinct but low dorsal flap (Fig. 3A–C, E–G; *cf.* Mitra and Waikhom, 2019: figs. 2A, B, E, F, 4A–C for *Po. palelensis*; Ng *et al.*, 2020: fig. 3D for *Po. whitteni*; personal observation for *Po. tumidulus*). *Potamiscus mima* sp. nov. and *Po. whitteni* are readily distinguishable from *Po. chizami* sp. nov., *Po. palelensis*, and *Po. tumidulus* by their relatively narrow male pleon (Fig. 2I, L; *cf.* Ng *et al.*, 2020: figs. 2A, B, 3A for *Po. whitteni*) (*vs.* relatively broad male pleon, Fig. 2C, F; *cf.* Mitra and Waikhom, 2019: fig. 1C for *Po. palelensis*; personal observation for *Po. tumidulus*) and the relatively more slender G1 terminal segment (Fig. 3E–G; *cf.* Ng *et al.*, 2020: fig. 3C–F for *Po. whitteni*) (relatively more stout G1 terminal segment, Fig. 3A–C; *cf.* Mitra and Waikhom, 2019: figs. 2A, B, E, F, 4A–C for *Po. palelensis*; personal observation for *Po. tumidulus*). On the other hand, *Po. mima* sp. nov. is distinct from *Po. whitteni* by its gently convex dorsal surface of the carapace (Fig. 2H) (*vs.* distinctly convex dorsal surface of the carapace; *cf.* Ng *et al.*, 2020: fig. 1D), a barely visible groove between epigastric- and postorbital cristae (Figs. 2G, 4D) (*vs.* distinct groove between epigastric- and postorbital cristae; *cf.* Ng *et al.*, 2020: fig. 1A–C), the separation of the suborbital margin from the supraorbital margin by the external orbital angle (Fig. 2H) (*vs.* confluent suborbital- and supraorbital margins; *cf.* Ng *et al.*, 2020: fig. 1D), the broader male pleonal somite 2 than somite 1 (Fig. 2L) (*vs.* equally broad male pleonal somites 1, 2; *cf.* Ng *et al.*, 2020: fig. 3A), the strongly concave lateral margins of the male telson (Fig. 2I, L) (*vs.* gently concave to almost straight lateral margins of the male telson; *cf.* Ng *et al.*, 2020: figs. 2A, B, 3A), and the straight G1 tip (Fig. 3E, F) (*vs.* upcurved G1 tip; *cf.* Ng *et al.*, 2020: fig. 3D, F).

In addition to the narrow male pleon and the slender G1 terminal segment, *Po. mima* sp. nov. is easily separated from *Po. palelensis* by its stouter ambulatory legs, P3 merus approximately 2.8 times long as broad (Figs. 2G, 4D) (*vs.* relatively slender ambulatory legs, P3 merus approximately 3.7 times long as broad; *cf.* Mitra and Waikhom, 2019: fig. 1A) and the gently curved distal third of the G1 terminal segment (Fig. 3E, F) (*vs.* distinctly curved distal third of the G1 terminal segment; *cf.* Mitra and Waikhom, 2019: figs. 2A, B, 4A, C).

Furthermore, *Po. mima* sp. nov. is differentiated from *Po. tumidulus* in many characters of the carapace, including postorbital cristae, external orbital angle, epibranchial tooth, suture between the male S3/S4,

and male sternopleonal cavity (see Remarks for *Po. chizami* sp. nov.).

Potamiscus mima sp. nov. and *Po. chizami* sp. nov. can be distinguished from each other as compared in the remarks for *Po. chizami* sp. nov.

Potamiscus mima sp. nov. need not be confused with some similar looking Indian species (*viz.*, *Po. annandali* and *Po. decourcyi*) due to its less bent (curved outwards at an angle of about 30° from the longitudinal axis of the G1) and relatively slender G1 terminal segment, which possesses a low but distinct dorsal flap (Fig. 3E–G). In addition to lacking a dorsal flap, *Po. annandali* and *Po. decourcyi* have a G1 terminal segment that is strongly bent (curved outwards at an angle of about 55° from the longitudinal axis of the G1) and relatively stout (*cf.* Bott, 1970: pl. 38, fig. 28 for *Po. annandali*; personal observation for *Po. decourcyi*).

Geographical distribution. *Potamiscus mima* sp. nov. is only known from Mima village in Kohima District of Nagaland, northeastern India.

Acknowledgements

The author thanks Dr. Kailash Chandra, Director (Zoological Survey of India, Kolkata) for support and research facilities. I am grateful to Mr. Wetetsho Kapfo, Research Fellow (Healthcare Laboratory & Research Centre, Naga Hospital Authority, Kohima, Nagaland, India) for making the material available for study. I would like to thank Dr. Peter K.L. Ng (National University of Singapore) for sharing necessary literature. Special thanks to Dr. Darren C.J. Yeo (National University of Singapore) and Dr. Santanu Mitra (Zoological Survey of India, Kolkata) for sharing the images of some type material. I gratefully acknowledge three anonymous reviewers for their constructive comments and valuable suggestions.

References

Bott, R. 1970. Die Süßwasserkrabben von Europa, Asien, Australien und ihre Stammesgeschichte. Eine Revision der Potamoidea und Parathelphusoidea (Crustacea, Decapoda). *Abhandlungen der Senckenbergischen Naturforschenden Gesellschaft*, 526: 1–338.

Chu, K.; Zhou, L. and Sun, H. 2017. A new genus and new species of freshwater crab (Decapoda: Brachyura: Potamidae Ortmann, 1896) from Yunnan Province, China. *Zootaxa*, 4286: 241–253.

Coleman, C.O. 2018. Shadings in digital taxonomic drawings. *Zoosystematics and Evolution*, 94: 529–533.

Dai, A.Y. 1999. Fauna Sinica: Arthropoda: Crustacea: Malacostraca: Decapoda: Parathelphusidae, Potamidae. Beijing, Science Press, xiii+501p. [In Chinese with English abstract.]

Dai, A.Y. and Cai, Y.X. 1998. Freshwater crabs of Xishangbanna, Yunnan Province, China (Malacostraca: Crustacea: Parathelphusidae, Potamidae). *Acta Zootaxonomica Sinica*, 23: 245–251. [In Chinese with English abstract.]

Davie, P.J.F.; Guinot, D. and Ng, P.K.L. 2015. Anatomy and functional morphology of Brachyura. p. 11–163. In: P. Castro; P.J.F. Davie; D. Guinot; F.R. Schram and J.C. von Vaupel Klein (eds), Treatise on Zoology – Anatomy, Taxonomy, Biology. The Crustacea. Volume 9 (Part C-I). Decapoda: Brachyura (Part 1). Leiden, Brill.

Mitra, S. 2019. A new species of *Himalayapotamon* Pretzmann, 1966 (Decapoda: Brachyura: Potamidae: Potaminae) from Western Himalaya, India. *Journal of Environment & Sociobiology*, 16: 121–131.

Mitra, S. and Waikhom, M.D. 2019. A new species of freshwater crab of the genus *Potamiscus* Alcock, 1909 (Crustacea: Brachyura: Potamidae: Potamiscinae) from Manipur, north-eastern India. *Journal of Emerging Technologies and Innovative Research*, 6: 624–634.

Mitra, S.; Payra, A. and Chandra, K. 2018. A new species of freshwater crab of the genus *Teretamon* Yeo & Ng, 2007 (Decapoda: Brachyura: Potamidae) from Arunachal Pradesh, northeastern India. *Zootaxa*, 4500: 587–595.

Montesanto, G. 2015. A fast GNU method to draw accurate scientific illustrations for taxonomy. *ZooKeys*, 515: 191–206.

Montesanto, G. 2016. Drawing setae: a GNU way for digital scientific illustrations. *Nauplius*, 24: e2016017.

Naruse, T.; Chia, J.E. and Zhou, X. 2018. Biodiversity surveys reveal eight new species of freshwater crabs (Decapoda: Brachyura: Potamidae) from Yunnan Province, China. *PeerJ*, 6: e5497.

Ng, P.K.L. 1988. The freshwater crabs of Peninsular Malaysia and Singapore. Singapore, Department of Zoology, National University of Singapore, Shinglee Press, 156p.

Ng, P.K.L.; Guinot, D. and Davie, P.J.F. 2008. Systema Brachyurorum: Part I. An annotated checklist of extant brachyuran crabs of the world. *Raffles Bulletin of Zoology*, Supplement 17: 1–286.

Ng, P.K.L.; Htoo, H. and Win Mar. 2020. *Potamiscus whitteni*, a new freshwater crab from Chin State, Myanmar (Crustacea: Brachyura: Potamidae). *Raffles Bulletin of Zoology*, Supplement 35: 129–136.

Pati, S.K. and Thackeray, T. 2018. The freshwater crab genera *Ghatiana* Pati & Sharma, *Gubernatoriana* Bott, and *Inglethelphusa* Bott (Crustacea: Decapoda: Brachyura: Gecarcinucidae) revisited, with descriptions of a new genus and eleven new species. *Zootaxa*, 4440: 1–73.

Pati, S.K.; Mitra, S. and Yeo, D.C.J. 2019a. A new species of *Acanthopotamon* Kemp, 1918 (Decapoda: Brachyura: Potamidae: Potaminae) from northeastern India, with a key to the species of the genus and notes on their distribution in relation to freshwater ecoregions. *Journal of Crustacean Biology*, 39: 450–458.

Pati, S.K.; Sujila, P.S. and Sudha Devi, A.R. 2019b. Description of a new species of freshwater crab of the genus *Arcithelphusa* Pati & Sudha Devi, 2015 (Decapoda: Brachyura: Gecarcinucidae) from the Western Ghats, Kerala, India. *Zootaxa*, 4674: 203–214.

Pati, S.K.; Yeo, D.C.J. and Ng, P.K.L. 2020. *Krishnamon*, a new genus for the cavernicolous crab *Telphusa austeniana* Wood-Mason, 1871 (Decapoda: Brachyura: Potamidae) from Meghalaya state, northeastern India. *Journal of Crustacean Biology*, 40: 301–308.

Shih, H.-T.; Yeo, D.C.J. and Ng, P.K.L. 2009. The collision of the Indian plate with Asia: molecular evidence for its impact on the phylogeny of freshwater crabs (Brachyura: Potamidae). *Journal of Biogeography*, 36: 703–719.

Türkay, M. and Naiyanetr, P. 1987. The identity of *Potamon rangoonense* Rathbun, 1904 and *Thelphusa larnaudii* A. Milne-Edwards 1869, with introduction of *Neolarnaudia botti* n. g. n. sp. (Crustacea: Decapoda: Potamidae). *Senckenbergiana biologica*, 67: 389–396.

Yeo, D.C.J. and Ng, P.K.L. 2004. Recognition of two subfamilies in the Potamidae Ortmann, 1896 (Brachyura, Potamidae) with a note on the genus *Potamon* Savigny, 1816. *Crustaceana*, 76: 1219–1235.

Zhang, Z.; Xing, Y.; Cheng, J.; Pan, D.; Lv, L.; Cumberlidge, N. and Sun, H. 2020. Phylogenetic implications of mitogenome rearrangements in East Asian potamiscine freshwater crabs (Brachyura: Potamidae). *Molecular phylogenetics and Evolution*, 143: 106669.